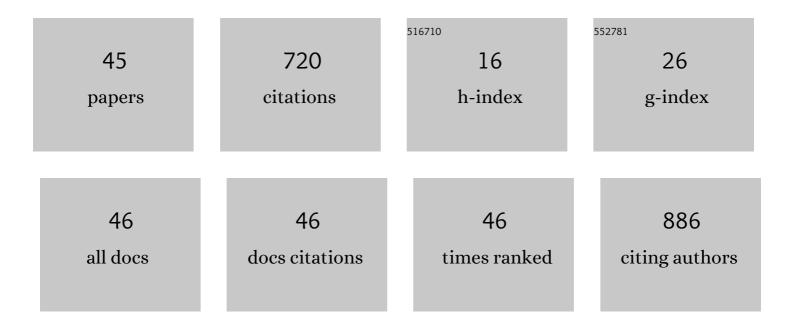
Ajeet Srivastav

List of Publications by Year in descending order

Source: https://exaly.com/author-pdf/1910111/publications.pdf Version: 2024-02-01



AIFET SDIVASTAV

#	Article	IF	CITATIONS
1	Magnetic nanowires by electrodeposition within templates. Physica Status Solidi (B): Basic Research, 2010, 247, 2364-2379.	1.5	139
2	On Joule heating during spark plasma sintering of metal powders. Scripta Materialia, 2014, 93, 52-55.	5.2	61
3	Graphene from discharged dry cell battery electrodes. Journal of Hazardous Materials, 2019, 366, 358-369.	12.4	45
4	Review: Oxygen-deficient tungsten oxides. Journal of Materials Science, 2021, 56, 6615-6644.	3.7	40
5	Grain-size-dependent non-monotonic lattice parameter variation in nanocrystalline W: The role of non-equilibrium grain boundary structure. Scripta Materialia, 2015, 98, 20-23.	5.2	36
6	Thermodynamic calculation and experimental validation of Hf-rich glass forming compositions in Hf-Cu-Ni system. Journal of Non-Crystalline Solids, 2018, 500, 191-195.	3.1	25
7	Initial-stage Sintering Kinetics of Nanocrystalline Tungsten. Metallurgical and Materials Transactions A: Physical Metallurgy and Materials Science, 2011, 42, 3863-3866.	2.2	24
8	In-situ \$\$hbox {TiO}_{2}\$\$ TiO 2 –rGO nanocomposites for CO gas sensing. Bulletin of Materials Science, 2018, 41, 1.	1.7	23
9	Loading Rate Sensitivity of Jute/Glass Hybrid Reinforced Epoxy Composites: Effect of Surface Modifications. Journal of Reinforced Plastics and Composites, 2007, 26, 851-860.	3.1	21
10	Crystal anisotropy induced temperature dependent magnetization in cobalt nanowires electrodeposited within alumina template. Journal of Magnetism and Magnetic Materials, 2014, 349, 21-26.	2.3	20
11	Localized pore evolution assisted densification during spark plasma sintering of nanocrystalline W-5wt.%Mo alloy. Scripta Materialia, 2019, 159, 41-45.	5.2	20
12	Crystallite size induced bandgap tuning in WO3 derived from nanocrystalline tungsten. Scripta Materialia, 2020, 176, 47-52.	5.2	20
13	Crystallographic-shear-phase-driven W18O49 nanowires growth on nanocrystalline W surfaces. Scripta Materialia, 2016, 115, 28-32.	5.2	19
14	Graphene/chitosan-functionalized iron oxide nanoparticles for biomedical applications. Journal of Materials Research, 2019, 34, 3389-3399.	2.6	17
15	Estimation of diffusivity from densification data obtained during spark plasma sintering. Scripta Materialia, 2019, 161, 36-39.	5.2	17
16	Molten salt electrolysis of neodymium: electrolyte selection and deposition mechanism. Institutions of Mining and Metallurgy Transactions Section C: Mineral Processing and Extractive Metallurgy, 2010, 119, 88-92.	0.6	16
17	XRD Characterization of Microstructural Evolution During Mechanical Alloying of W-20Âwt%Mo. Transactions of the Indian Institute of Metals, 2013, 66, 409-414.	1.5	16
18	Dilatometric analysis on shrinkage behavior during non-isothermal sintering of nanocrystalline tungsten mechanically alloyed with molybdenum. Journal of Alloys and Compounds, 2012, 536, S41-S44.	5.5	15

AJEET SRIVASTAV

#	Article	IF	CITATIONS
19	On correlation between densification kinetics during spark plasma sintering and compressive creep of B2 aluminides. Scripta Materialia, 2015, 107, 63-66.	5.2	15
20	Antioxidant efficacy of chitosan/graphene functionalized superparamagnetic iron oxide nanoparticles. Journal of Materials Science: Materials in Medicine, 2018, 29, 154.	3.6	14
21	Effect of Re on microstructural evolution and densification kinetics during spark plasma sintering of nanocrystalline W. Advanced Powder Technology, 2019, 30, 2779-2786.	4.1	14
22	Evolution of morphology and texture during high energy ball milling of Ni and Ni-5 wt%Cu powders. Materials Characterization, 2016, 120, 90-96.	4.4	10
23	Thermodynamic model to predict bulk metallic glass forming composition in Zr-Cu-Fe-Al system and understanding the role of Dy addition. Physica B: Condensed Matter, 2022, 624, 413416.	2.7	10
24	Measurements of the melting points, liquidus, and solidus of the Mo, Ta, and Mo Ta binary alloys using a novel high-speed pyrometric technique. International Journal of Refractory Metals and Hard Materials, 2020, 93, 105335.	3.8	9
25	Understanding the Growth Mechanism of Hematite Nanoparticles: The Role of Maghemite as an Intermediate Phase. Crystal Growth and Design, 2021, 21, 16-22.	3.0	9
26	Formation of amorphous alumina during sintering of nanocrystalline B2 aluminides. Materials Characterization, 2016, 119, 186-194.	4.4	7
27	Novel coalescence-driven grain-growth mechanism during annealing/spark plasma sintering of NiO nanocrystals. Journal of the European Ceramic Society, 2017, 37, 4973-4977.	5.7	7
28	Graphene-based chemiresistive gas sensors. Comprehensive Analytical Chemistry, 2020, , 149-173.	1.3	6
29	Unveiling the crystallographic origin of mechanochemically induced monoclinic to triclinic phase transformation in WO ₃ . CrystEngComm, 2021, 23, 1821-1827.	2.6	6
30	On the temperature dependent magnetization in dual-phase Co nanowires confinedly electrodeposited inside nanoporous alumina membrane. Journal of Crystal Growth, 2021, 562, 126084.	1.5	5
31	Understanding the strain-dependent structure of Cu nanocrystals in Ag–Cu nanoalloys. Physical Chemistry Chemical Physics, 2021, 23, 26165-26177.	2.8	5
32	Nucleation and growth mechanism of Co–Pt alloy nanowires electrodeposited within alumina template. Journal of Nanoparticle Research, 2015, 17, 1.	1.9	4
33	Kinetic Approach to Determine the Glass-Forming Ability in Hf-Based Metallic Glasses. Metallurgical and Materials Transactions A: Physical Metallurgy and Materials Science, 2021, 52, 1169-1173.	2.2	4
34	Formation mechanism of nanocrystalline W derived cubic-H0.5WO3. Scripta Materialia, 2022, 208, 114363.	5.2	4
35	Microstructure evolution and densification during spark plasma sintering of nanocrystalline W-5wt.%Ta alloy. Philosophical Magazine Letters, 2020, 100, 442-451.	1.2	3
36	Unraveling the growth mechanism of W18O49 nanowires on W surfaces. CrystEngComm, 2021, 23, 6559-6566.	2.6	3

AJEET SRIVASTAV

#	Article	IF	CITATIONS
37	Tribological and Morphological Evaluation of Ni-P and Ni-P/D Coatings. Materials Science Forum, 0, 969, 73-79.	0.3	2
38	WO3.1/3H2O nanorods/nanoplates: Growth mechanism and CO2 uptake. Materialia, 2020, 14, 100943.	2.7	2
39	Kinetics and phase formation during crystallization of Hf64Cu18Ni18 amorphous alloy. Phase Transitions, 2021, 94, 110-121.	1.3	2
40	Corrosion Studies of Hf64Cu18Ni18 Metallic Glass in Acidic and Alkaline Media. Transactions of the Indian Institute of Metals, 2021, 74, 949-956.	1.5	2
41	Modeling and Theory: general discussion. Faraday Discussions, 2016, 186, 371-398.	3.2	1
42	Applications to Soft Matter: general discussion. Faraday Discussions, 2016, 186, 503-527.	3.2	1
43	Nanocomposites: general discussion. Faraday Discussions, 2016, 186, 277-293.	3.2	1
44	Synthesis of Nanoparticle Assemblies: general discussion. Faraday Discussions, 2016, 186, 123-152.	3.2	0
45	Applicability of γ* Parameter on Glass Forming Ability of Zr-,Ti-,Hf-(Cu–Ni)-based Metallic Glasses. Transactions of the Indian Institute of Metals, 2018, 71, 2839-2843.	1.5	0